Available online at www.sciencedirect.com
SCIENCE DIRECT®
Polymer 44 (2003) 5303–5310
polymer
www.elsevier.com/locate/polymer

Association and physical gelation of ABA triblock copolymer in selective solvent

Katsuhiro Inomata[a,*], Daisuke Nakanishi[a], Ai Banno[a], Eiji Nakanishi[a], Yosuke Abe[b], Ryuta Kurihara[b], Kentaro Fujimoto[b], Takuhei Nose[c]

[a]*Department of Materials Science and Engineering, Nagoya Institute of Technology, Gokiso-cho, Showa-ku, Nagoya 466-8555, Japan*
[b]*Department of Polymer Chemistry, Tokyo Institute of Technology, 2-12-1 Ookayama, Meguro-ku, Tokyo 152-8552, Japan*
[c]*Department of Applied Chemistry, Tokyo Institute of Polytechnics, Iiyama, Atsugi 243-0297, Japan*

Received 6 January 2003; received in revised form 6 May 2003; accepted 20 June 2003

Abstract

Association behavior and physical gelation mechanism of ABA triblock copolymer dissolved in B-selective solvent have been studied systematically from dilute to moderately concentrated solutions. Static and dynamic light scattering and nuclear magnetic resonance measurements for dilute solutions of poly(methyl methacrylate)-*block*-poly(*tert*-butyl acrylate)-*block*-poly(methyl methacrylate) (PMMA–P*t*BuA–PMMA) in 1-butanol (P*t*BuA selective solvent) indicated that PMMA–P*t*BuA–PMMA chains are molecularly dissolved above 50 °C. With decreasing temperature, the triblock copolymers form associated micelles consisting PMMA associated core and P*t*BuA shell. Linear dynamic viscoelastic measurements for solutions with moderate concentration (3.9–12.0 wt%) revealed that the system was viscous sol state at 60 °C. Drastic increase of shear storage modulus (G') occurred with decreasing temperature, and at 25 °C, G' showed rubbery plateau with weak frequency dependency, means the formation of elastic physical gel. The consistency between the temperature for micelle formation and that at the increase in G' indicates that the physical gelation is owing to the network formation as the result of the association of PMMA chains and the bridging P*t*BuA chains connecting the PMMA cores. Master curves for the dynamic moduli were derived by time–temperature superposition along the frequency axis. Just above sol–gel transition concentration (C_{gel}), the master curves suggest the existence of fairy amount of aggregate that is not incorporated in the macroscopic network. With the increase in polymer concentration, the master curves become to reveal Maxwell-type viscoelasticity with narrow relaxation time distribution, suggesting the formation of transient network with easily generation and destruction of crosslinks. Concentration dependency of the plateau modulus is stronger than the theoretically expected, means the macroscopic transient network grows with polymer concentration by increasing the fraction of elastically effective bridging P*t*BuA chain above C_{gel}.

Keywords: ABA triblock copolymer; Association; Physical gel

1. Introduction

ABA triblock copolymer having long middle B block and short A blocks is widely used as thermoplastic elastmers, in which A blocks form hard microdomains by microphase separation, and the A domain and B chain act as crosslinking point and bridging chain, respectively. In a selective solvent, which is a good solvent for B block and a poor or bad solvent for A block, the ABA triblock copolymer forms associate or micelle as a consequence of association of poorly-soluble A block. When the concentration is very low and the copolymer forms isolated flower-like micelles, the B block chain takes loop conformation with the both-end A blocks incorporated in the same associated micellar core. With the increase of the copolymer concentration, the probability that respective A blocks in one copolymer are incorporated in different associated cores will increase. In this case, the middle B block can possibly take two conformations: one is the loop conformation as like that in the isolated micelle, and the other is bridge conformation that connects two different associates. The increase of the bridge conformation will induce the formation of organized network consisting of A-chain-associated crosslinking points and bridging B chains. If the

* Corresponding author. Tel./fax: +81-52-735-5274.
E-mail address: inomata@mse.nitech.ac.jp (K. Inomata).

0032-3861/03/$ - see front matter © 2003 Elsevier Ltd. All rights reserved.
doi:10.1016/S0032-3861(03)00534-2

association strength of A chain is weak and A chains are allowed to reversibly associate to or dissociate from the crosslinking point, the viscoelastic properties of this transient network strongly depend on a finite dissociation time.

Theoretical consideration of the transient network was first presented by Green and Tobolsky [1], in which the rubber elasticity was extended so as to allow for the creation and annihilation of junctions during the network deformation. Tanaka and Edwards [2–6] presented a transient network theory with considering a molecular picture of telechelic polymers having associative groups at their chain ends. They focused on the unentangled regime where each polymer chain has smaller molecular weight than the entanglement molecular weight and obeys Rouse dynamics. When the associated A chain is dissociated from the junction either by their own thermal motion or by being pulled by tension, it must be necessary to overcome the potential barrier W for A chain to dissociate. Therefore, the probability for this dissociation process is proportional to $\exp(-W/kT)$ where k and T are the Boltzmann constant and the absolute temperature, respectively. The calculated dynamic mechanical modulus vs. frequency curve resembled with conventional Maxwell-type viscoelastic curve with single relaxation time [4]. Their theory is suitable to describe the transient networks made up of ABA triblock copolymers in which crosslinks are generated and destroyed by the association and dissociation of A chains.

Because of its importance in industrial use, experimental investigations for structures and dynamics of physical gels by ABA triblock copolymers in selective solvent have been extensively reported [7–23]. In case of the physical gels of polystyrene-*block*-polyisoprene-*block*-polystyrene (SIS), hydrocarbons such as tetradecane and *n*-heptane are used as selective solvent for the middle polyisoprene block [13–21]. These hydrocarbons are almost non-solvent for the terminal polystyrene (PS) block, and then, PS chains are usually fixed in the associated core even though the core is not in glassy state. In this sense, SIS/hydrocarbon system cannot be regarded as the transient network because the recombination of the crosslinks is hardly expected. In order to achieve the state that the association and dissociation of the micelle core will easily occur, it is suitable to conduct the experiments near critical micelle temperature ($T_{micelle}$) at which the association strength of the terminal block is not strong enough and the core is swollen by solvent. However, there have been very few systematic investigations from dilute solution to moderately concentrated solution above sol–gel transition concentration (C_{gel}) near $T_{micelle}$, in order for understanding the structures and dynamics of the transient network by ABA triblock copolymers.

In this study, we report the association behavior and viscoelastic properties of ABA triblock copolymer solution, poly(methyl methacrylate)-*block*-poly(*tert*-butyl acrylate)-*block*-poly(methyl methacrylate) (PMMA–P*t*BuA–PMMA) dissolved in 1-butanol. 1-Butanol is a good solvent for P*t*BuA block but a poor solvent for PMMA block. The used PMMA–P*t*BuA–PMMA in this study has relatively short PMMA blocks at the both end of longer P*t*BuA block, and is expected to form an associated PMMA core with the well-dissolved P*t*BuA chains in 1-butanol. Because of the similarity in the chemical structure of PMMA and P*t*BuA, the solvent quality of 1-butanol for PMMA block is not so bad. As will be described later in Section 3, PMMA–P*t*BuA–PMMA/1-butanol dilute solution has $T_{micelle}$ around 45–50 °C, and we can conduct the viscoelasticity measurements for moderately concentrated solutions (3.0–12.0 wt%) above and below C_{gel} by changing temperature (25–60 °C) near $T_{micelle}$. Comparison of the sol–gel transition temperature with $T_{micelle}$ reveals the molecular origin for the formation of the transient network. Growth mechanism of the macroscopic network will be discussed by the concentration and temperature dependencies of the linear dynamic viscoelasticity.

2. Experiments

2.1. Materials and samples

Triblock copolymer, PMMA–P*t*BuA–PMMA, was purchased from Polymer Source Inc., and used as received. The authorized number-averaged molecular weight (M_n) for PMMA and P*t*BuA blocks are 10,400 and 49,500, respectively. The total M_n, molecular weight distribution index M_w/M_n, and PMMA weight fraction is 70,300, 1.16, and 0.30, respectively. Poly(*tert*-butyl acrylate) homopolymer, designated as H-P*t*BuA, was also purchased from Polymer Source Inc., and used as received. The authorized M_n and M_w/M_n are 79,000 and 1.30, respectively. 1-Butanol, as selective solvent to P*t*BuA, was a HPLC grade product of Aldrich, and used without further purification. For ^{1}H NMR measurements, deuterated solvent 1-butanol-d_{10} was purchased from Aldrich and used without purification.

Sample solutions for light scattering and viscoelastic measurements were prepared as follows. 1-Butanol solutions with desired polymer concentrations ranging from 0.49 to 12.0 wt% were homogenized by stirring for 1 h at 100 °C and subsequently cooled down to room temperature. The prepared solutions were left standing at least for one night before measurements.

2.2. Measurements

2.2.1. ^{1}H NMR

^{1}H NMR spectra were recorded on a JEOL GSX500 spectrometer operating at 500 MHz. Toluene solution of PMMA–P*t*BuA–PMMA was filtered and transferred into 5-mm outer diameter NMR tube. After complete evacuation of toluene under vacuum, Millipore-filtered 1-butanol-d_{10} was added, and the tube was flame-sealed under gentle

vacuum. The polymer concentration was 0.54 wt%. At first, the solution was maintained at 100 °C in the NMR apparatus, and subsequently NMR spectra were measured with decreasing temperature from 100 to 30 °C. The solvent peaks were used as a reference for the chemical shift, calibrated by tetramethylsilane/1-butanol-d_{10} solution.

2.2.2. Light scattering

Light scattering was measured by a laboratory-made apparatus equipped with an ALV/SO-SIPD detector and an ALV-5000 correlator using He–Ne laser (the wavelength of 633 nm) as a light source [24,25]. Sample solution with the polymer concentration of 0.49 wt% was optically purified by a Millipore filter of nominal pore size of 0.45 μm and transferred into optical tube, and the tube was flame-sealed under gentle vacuum. The solution was maintained at 100 °C in oil bath of the apparatus, subsequently the temperature was decreased, and the light scattering measurements were performed at desired temperature between 25 to 100 °C.

The excess Rayleigh ratio $R(\theta)$ was calculated from the measured excess scattering intensity as a function of scattering angle θ. Since the extrapolation to the dilute limit was not available because of the association, the apparent molecular weight $M_{w,app}$ and apparent radius of gyration $R_{g,app}$ were evaluated without extrapolation to zero concentration. These are defined as

$$M_{w,app} = R(0)/KC \tag{1}$$

$$R^2_{g,app} = 3\lambda_0^2 M_{w,app}(\text{initial slope})/16\pi^2 n^2 \tag{2}$$

where the constant K is given by

$$K = 4\pi^2 n^2 (\partial n/\partial C)^2/(N_A \lambda_0^4) \tag{3}$$

with n being the refractive index of the solvent, N_A the Avogadro constant, $\partial n/\partial C$ the refractive index increment, and λ_0 the wavelength of the incident light in vacuum. $KC/R(0)$ and (initial slope) are the intercept and the initial slope of $KC/R(\theta)$ vs. $\sin^2(\theta/2)$ plot at a finite concentration. The refractive index increment was measured by a differential refractometer (RM-102, UNION Giken) as a function of temperature t, and obtained as

$$(\partial n/\partial C)/(\text{ml/g}) = 0.0762 - 0.00019(t/°\text{C}) \tag{4}$$

The correlation function of the electric field obtained from the auto-correlation function of the scattered light intensity on the basis of the homodyne scattering exhibited a unimodal decay, and allowed us to obtain the decay rate Γ by the second-order cumulant method. The decay rate was transformed to the diffusion coefficient D by

$$D = \Gamma/q^2 \tag{5}$$

where q is the wave number given by

$$q = (4\pi n/\lambda_0)\sin(\theta/2) \tag{6}$$

The obtained D values are apparent one, D_{app}, because of the same reason for the static light scattering. D_{app} was further transformed to the apparent hydrodynamic radius $R_{h,app}$ by using the Einstein–Stokes equation

$$R_{h,app} = kT/(6\pi\eta D_{app}) \tag{7}$$

where η is solvent viscosity.

2.2.3. Linear dynamic viscoelasticity

The dynamic viscoelasticity was measured with an ARES viscoelastic measuring apparatus (Rheometrics) using cone-plate fixture with diameter of 25 mm and cone angle of 0.04 rad. In order to prevent from solvent evaporation and keep the temperature as precise as possible, a specially designed cover and solvent trap were made and properly installed surrounding the rotator holding sample solution [24]. No detectable solvent evaporation was found after several-hours measurement at temperatures up to 50 °C. The sample temperature was measured by platinum resistive thermometer touched at the bottom of the lower fixture (plate jig), and controlled by outer water circulator and bath in which the lower fixture is mounted. PMMA–P*t*BuA–PMMA/1-butanol systems above 3.9 wt% polymer concentration are gel-like at room temperature, and it was difficult to install a proper amount of gel-like sample between the cone and plate fixture without residual stress. Hence, the sample solution and apparatus was heated at 60 °C in advance, and installed the solution between the cone and plate as rapid as possible in order to prevent from solvent evaporation.

All the measurements were performed within the linear viscoelasticity, which was confirmed by no strain dependence of the dynamic shear storage modulus $G'(\omega)$ and loss modulus $G''(\omega)$, where ω is an angular frequency. The strain ranged from 0.01 to 0.5 depending on the concentration and temperature of the solution. The dynamic modulus was measured at various temperatures of 25–60 °C upon cooling process.

3. Results

3.1. Micellization in dilute solutions observed by ^{1}H NMR and light scattering measurements

Fig. 1 shows the temperature dependence of ^{1}H NMR spectra for PMMA–P*t*BuA–PMMA/1-butanol-d_{10} solution with the concentration of 0.54 wt%. A broad peak around 2.3 ppm, which is overlapped with an impurity signal, can be assigned to the methine protons in P*t*BuA block. The peak gradually tends to be broad with decreasing temperature, but is still observed at 30 °C. On the other hand, the peak intensity for the methoxy protons in PMMA block, appears at 3.6–3.7 ppm, decreases rapidly with decreasing temperature. At 30 °C, it is difficult to distinguish the existence of the peak, which suggests the decrease of the mobility of PMMA chain. With considering the solubility of

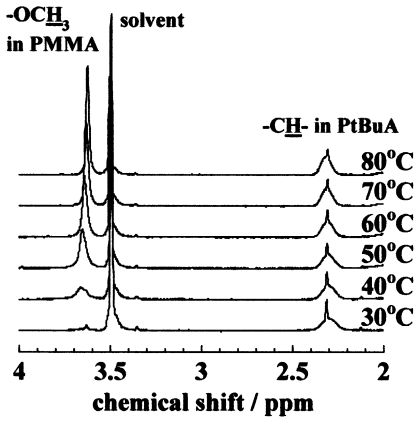

Fig. 1. NMR spectra for methine protons in P*t*BuA block and methoxy protons in PMMA block observed for PMMA–P*t*BuA–PMMA/1-butanol-d_{10} solution with 0.54 wt% at each indicated temperature.

PMMA and P*t*BuA chains in 1-butanol, it is plausible that PMMA–P*t*BuA–PMMA chains form an associate with dissolved P*t*BuA chains and PMMA concentrated domains. In Fig. 2, the relative value of integrated intensity of the methoxy protons in PMMA block to that of the methine protons in P*t*BuA block, I_{PMMA}/I_{PtBuA}, is plotted against temperature. I_{PMMA}/I_{PtBuA} is almost constant above 60 °C, and monotonously decreases with decreasing temperature from 60 to 30 °C. These results indicate that the association strength of PMMA chains in 1-butanol increases due to the solvent quality getting worse with the decrease of temperature.

Static and dynamic light scattering measurements were performed upon cooling from 100 to 25 °C. Fig. 3 shows the temperature dependence of the evaluated $M_{w,app}$, $R_{g,app}$, and $R_{h,app}$. At temperature higher than 45 °C, the scattering intensity is too weak to determine $R_{g,app}$ and $R_{h,app}$ precisely. The apparent molecular weight $M_{w,app}$ at temperatures higher than 50 °C is 1.1–1.5 times as larger than the nominal $M_w = M_n \times (M_w/M_n)$ of PMMA–P*t*BuA–PMMA, indicating that the polymer is dissolved in 1-butanol almost molecularly. Below 45 °C, $M_{w,app}$ starts to increase with

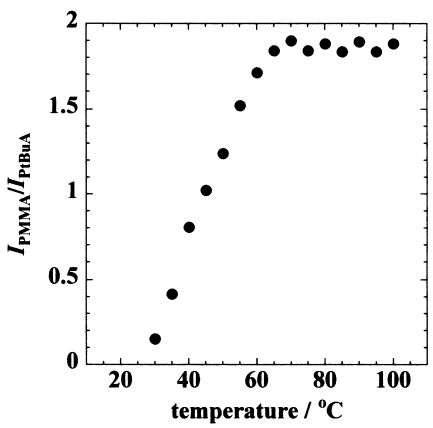

Fig. 2. Temperature dependence of the ratio of I_{PMMA} to I_{PtBuA}, which are integrated intensity of NMR peaks for methoxy and methine protons in PMMA and P*t*BuA blocks, respectively.

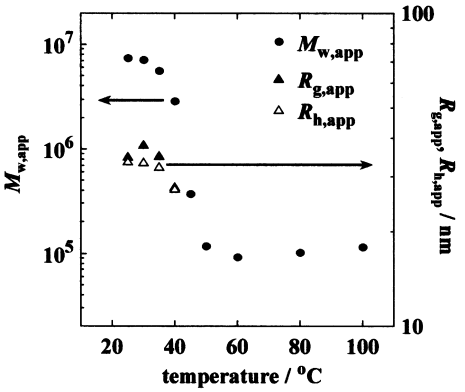

Fig. 3. Temperature dependence of $M_{w,app}$, $R_{g,app}$, and $R_{h,app}$ for 0.49 wt% PMMA–P*t*BuA–PMMA/1-butanol solution evaluated by static and dynamic light scattering measurements.

decreasing temperature, and approaches the almost constant value at 30 °C. At 25 °C, the apparent aggregation number, i.e. $M_{w,app}/M_w$, is obtained as 91. The similar temperature dependence is also recognized for $R_{g,app}$ and $R_{h,app}$. The value of $R_{g,app}/R_{h,app}$, which is an index for the particle shape, is ranged from 1.1 to 1.2 at the temperatures of 25–40 °C. This value is comparable to that of the star-shaped polymer (1.1–1.5), and less than those for random-coil (1.5–1.8) and rod-like chain (5 at long and thin limit). Therefore, PMMA–P*t*BuA–PMMA molecules in 1-butanol are believed to form core-corona type flower-like micelle with PMMA-associated core and P*t*BuA in loop conformation as corona at the temperature lower than $T_{micelle}$ around 45–50 °C.

3.2. Physical gelation observed by linear dynamic viscoelasticity

Temperature dependence of $G'(\omega)$ and $G''(\omega)$ was measured for solutions with 3.0, 3.9, 4.4, 5.9, 8.0, and 12.0 wt%. It should be noted that these systems were clear by visual observation in the range of 25–80 °C; no macrophase separation into polymer-rich and polymer-poor phases was recognized. Typical examples of the log–log plot of $G'(\omega)$ and $G''(\omega)$ against ω is shown in Fig. 4 for 3.0, 4.4, and 8.0 wt% solutions. In Fig. 4b for 4.4 wt% system, $G'(\omega)$ is smaller than $G''(\omega)$ at 60 and 50 °C in the measured ω region, and the slopes for $G'(\omega)$ and $G''(\omega)$ against ω are 2 and 1, respectively, indicating a viscous liquid at these temperatures. By further cooling below 50 °C, both shear moduli, especially $G'(\omega)$, exhibit sharp increase, and crossing point of $G'(\omega)$ and $G''(\omega)$ curves at larger ω region is appeared at 40 °C. At 35 °C the crossing point shifts to lower ω region, and below 30 °C, both moduli show weak dependency on temperature and on frequency, and $G'(\omega) \cong 40$ Pa $\gg G''(\omega)$. Here, the PMMA–P*t*BuA–PMMA/1-butanol system is rubbery, i.e. gel-like state in the frequency region of 0.1 rad/s $\leq \omega \leq$ 63.1 rad/s.

Similar temperature dependences of $G'(\omega)$ and $G''(\omega)$ are also observed for higher concentration, except that the

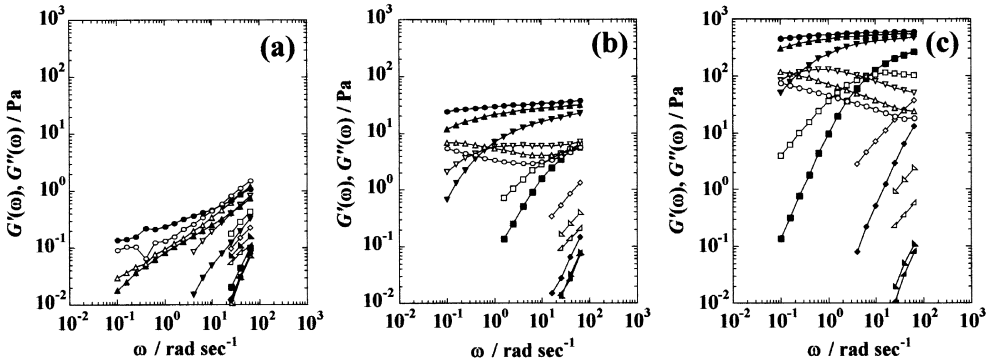

Fig. 4. Linear dynamic viscoelastic curves for (a) 3.0 wt%, (b) 4.4 wt%, and (c) 8.0 wt% solutions. Closed and open symbols are storage and loss modulus, respectively. Measurements were performed at 60 °C (◢,◿), 50 °C (◣,◺), 45 °C (◆,◇), 40 °C (■,□), 35 °C (▼,▽), 30 °C (▲,△), and 25 °C (●,○).

plateau G' value increases with polymer concentration. In 3.0 wt% solution (Fig. 4a), however, the region for $G' \gg G''$ is not observed and there is no distinct rubbery plateau, suggesting that the concentration of 3.0 wt% is lower than C_{gel}.

In Fig. 5, G' and G'' at the fixed ω (= 63.1 rad/s) are plotted against temperature for PMMA–P*t*BuA–PMMA/1-butanol system with various concentrations. In Fig. 5a for 3.9–5.9 wt%, $G' < G''$ at high temperature and both moduli increase sharply with decreasing temperature from 45 to 40 °C. After crossing around 39–41 °C, G' becomes larger than G'' and approaches a constant value. We can compare these plots with the temperature dependence of $M_{w,app}$ for dilute solution in Fig. 3, in which $M_{w,app}$ value shows sharp increase with cooling from 50 to 45 °C. Comparison of these temperatures strongly suggests that the change from sol to gel is attributed to the association of PMMA block; by the association, a macroscopically organized network is formed with consisting PMMA-segregated crosslinking points and bridging P*t*BuA chains. For higher concentration systems in Fig. 5b, the temperature at the sudden increase in G' is higher than that for the lower concentration, i.e. 45–50 °C for 8.0 wt% and 50–60 °C for 12.0 wt%.

Fig. 6a and b is the temperature dependence of dynamic viscosity $\eta' = G''/\omega$ for ABA triblock copolymer and H-P*t*BuA solutions, respectively, with 4.4 wt%. At 60 °C, ω-dependences of η' for both solutions are very weak with their values are less than 0.1 Poise. On decreasing temperature for the triblock copolymer system, η' increases drastically and shows distinct ω-dependence at 40 °C, i.e. the system is non-Newtonian fluid. On the other hand, for the homopolymer solution H-P*t*BuA/1-butanol, the temperature and the frequency dependences of η' are very weak within the range of 25–60 °C. These results also indicate that the existence of PMMA blocks is responsible to form the physical gel.

4. Discussion

The dynamic moduli for 3.0 wt% solution, which is lower than C_{gel}, are expressed by $G' \sim \omega^2$ and $G'' \sim \omega^1$ above 45 °C, but both exponent values become smaller with lowering temperature, means the system is non-Newtonian fluid. As shown in Fig. 7, the viscoelasticity at 30 °C in high-ω region is expressed as $G'(\omega) \sim G''(\omega) \sim \omega^{0.7}$, and the exponent value of 0.7 is close to that reported for sol–gel transition behavior of ABA triblock copolymer solution by Yu et al. [22]. Therefore, the concentration and temperature for Fig. 7 may be very close to the gelation point. It should be plausible that the concentration of 3.0 wt% is not enough to form a macroscopically organized

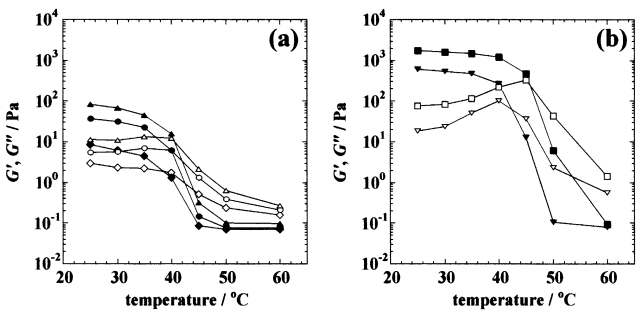

Fig. 5. Temperature dependence of G' (closed) and G'' (open); (a) 3.9 wt% (◆,◇), 4.4 wt% (●,○), and 5.9 wt% (▲,△) solutions; (b) 8.0 wt% (▼,▽) and 12.0 wt% (■,□) solutions.

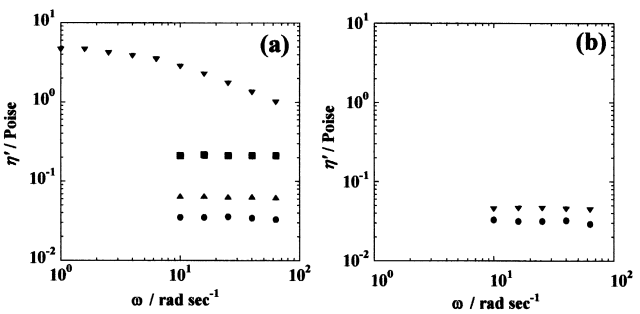

Fig. 6. Dynamic viscosity η' for 4.4 wt% solution of (a) PMMA–P*t*BuA–PMMA/1-butanol system and (b) H-P*t*BuA/1-butanol system measured at 60 °C (●), 50 °C (▲), 45 °C (■), and 40 °C (▼).

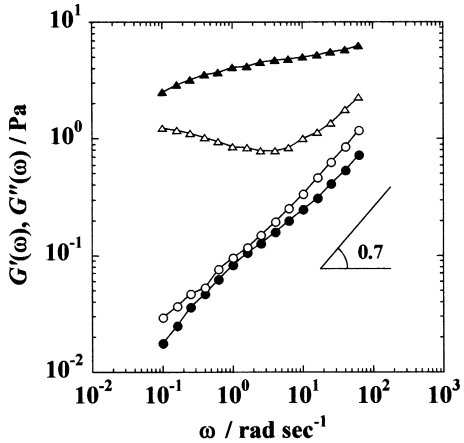

Fig. 7. Linear dynamic viscoelastic curves for 3.0 wt% (●,○) and 3.9 wt% (▲,△) solutions at 30 °C. Closed and open symbols represent $G'(\omega)$ and $G''(\omega)$, respectively.

network and that the system behaves like a solution of high-molecular-weight aggregate contains multiple micelles connected by the bridging P*t*BuA chains. In the viscoelastic curves for solutions above C_{gel}, similar ω-dependence of G'' is also recognized in high ω region and G' shows weak but obvious ω dependence, as shown in Fig. 7. Even though 3.9, 4.4, and 5.9 wt% systems show rubbery plateau at low temperature, they still contain fair amount of aggregates not incorporated in the macroscopically developed network, and their existence is considered to be giving influence on the viscoelasticity. On increasing the polymer concentration, the influence from the aggregates become negligible, and the rubbery elastic properties are dominant.

Fig. 8 shows master curves of G' and G'' referenced to 40 °C for 4.4–12.0 wt% solutions. These master curves were constructed by time–temperature superposition by shifting the modulus curves at each temperature along the frequency axis as G' values be superposed, and no shift along the modulus axis was applied. G'' curves at high temperature could not be superposed, so the master curves

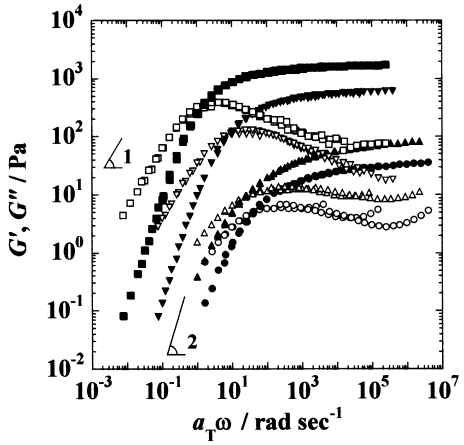

Fig. 8. Master curves for dynamic viscoelastic moduli derived after time–temperature superposition without modulus shift. (●,○) 4.4 wt%, (▲,△) 5.9 wt%, (▼,▽) 8.0 wt%, and (■,□) 12.0 wt%.

were constructed by using the modulus at 25–40 °C for 4.4 and 5.9 wt%, 25–45 °C for 8.0 wt%, and 25–50 °C for 12.0 wt%. Probably because of the existence of the above mentioned aggregates not incorporated in the macroscopic network, a well-superposed master curve was not obtained for 3.0 and 3.9 wt% solutions, and the superposition of G'' for 4.4 and 5.9 wt% systems was poor in the high ω region. For higher concentration systems with 8.0 and 12.0 wt%, G' curves show distinct rubbery-plateau at high frequency, and in low ω region, the dynamic moduli are scaled as $G' \sim \omega^2$ and $G'' \sim \omega^1$, means the terminal relaxation behavior. It should be pointed out that the same ω dependences of G' and G'' were also observed at higher temperature, but these moduli could not be superposed with the master curve for lower temperatures only by the shift along the frequency axis. This result indicates that the relaxation mechanisms for high and low temperature are different, and structural change with decreasing temperature can be considered as follows: at higher temperature, the triblock copolymers are almost molecularly dissolved in 1-butanol as suggested by the similarity of η' for PMMA–P*t*BuA–PMMA and H-P*t*BuA at 60 °C (Fig. 6), but at lower temperature the macroscopic network structure will be formed by the association of PMMA, and this is not identical with the molecularly dissolved state above $T_{micelle}$. The terminal relaxation behavior in the master curve means that the associating network can flow at high temperature, i.e. when the association strength of PMMA is weak enough. These master curves in Fig. 8 are similar to the Maxwell-type viscoelasticity with narrow relaxation time distribution, suggesting that PMMA–P*t*BuAMMA/1-butanol gels can be described by the transient network as described in Section 1 [4]. It may be pointed out that the detachment of PMMA chains from the associated core dominates the terminal flow behavior of the transient network in PMMA–P*t*BuA–PMMA/1-butanol system. G'' curves in high ω region, in contrast to the low ω region, do not obey the power law of $G'' \sim \omega^{-1}$, probably because of the distribution of the time constant for dissociation of PMMA chains from the associated core.

As shown in Fig. 5a, G' value starts to increase with decreasing temperature from 45 to 40 °C when the concentration is relatively low. This temperature, T_{VE}, is lower than $T_{micelle}$ for dilute solution (Fig. 3, 45–50 °C) and that when ^{1}H NMR signal intensity for PMMA block starts to decrease (Fig. 2, $60 < T_{NMR} < 65$ °C). The relationship of $T_{NMR} > T_{micelle} > T_{VE}$ can be described by the association and gelation behavior of PMMA–P*t*BuA–PMMA. At high temperature above T_{NMR}, solubility of PMMA chain in 1-butanol is not so bad and PMMA is well dissolved. With decreasing temperature, the solvent quality for PMMA becomes poor and the chain becomes less swollen, which induce the decrease in molecular mobility and also in NMR signal intensity. Further decrease in temperature induces the association of PMMA at $T_{micelle}$. However, the number density of micelle is not enough to form the organized

network just below $T_{micelle}$, and the whole system changes from sol to gel by linking micelles to form macroscopic network below T_{VE}. These explanations show how the transient network grow with decreasing temperature. The value of T_{VE} increased with polymer concentration, and at 12.0 wt%, G' value exhibits drastic increase between 50 and 60 °C. One possible reason for this observation is that $T_{micelle}$ depends on concentration, and the other is that there are enough micelles to form the macroscopic network just below $T_{micelle}$. Structural investigations for the positional correlation of micelles by small-angle X-ray scattering technique are in progress.

From the shift factor, a_T, along the frequency axis to obtain the master curves, we can evaluate the apparent activation energy (ΔH_{app}) from $\log(a_T)$ vs. $(1/T)$ plot. Typical Arrhenius plot for 5.9 wt% solution are shown in Fig. 9, and the evaluated ΔH_{app} values are listed in Table 1. These values are larger than the reported activation energy for aqueous solution of poly(ethylene glycol) with terminal alkyl chains (~70 kJ/mol) [7,8] or styrenic triblock copolymers (~200 kJ/mol) [21]. In the transient network theory [4], the activation energy corresponds to the energy barrier when the terminal chain is pulled out from the associated core. The energy barrier should be influenced by the segregation power of PMMA in 1-butanol. The temperature dependency of NMR spectra (Fig. 1) shows that PMMA chain mobility becomes worse steadily with decreasing temperature. This effect could contribute to the large ΔH_{app} value derived from the time–temperature shift.

The plateau modulus G_N^0 was evaluated as the G' value at $\omega = 63.1$ rad/s and 25 °C, and plotted against the polymer concentration, c, in the unit of g/ml in Fig. 10. The transient network theory predicts that the plateau modulus is given by $G_N^0 = \nu_0 kT$, where ν_0 is the number density of the elastically effective chains [1–6]. Here, we evaluate a fraction of elastically effective chains defined as $n_{eff} = G_N^0/\nu kT$, where ν is the number density of PMMA–P*t*BuA–PMMA chain in the solution. If the all P*t*BuA chains in solution act as bridging chain, G_N^0 will increase linearly with concentration and the value of n_{eff} should be equal to unity. The scaling exponent for G_N^0 against c, however, is much larger value than the expected one, i.e. $G_N^0 \sim c^{3.9}$ as shown in Fig. 10. The value of n_{eff} gradually approaches to 1 with the increase of polymer concentration, suggesting that only a few P*t*BuA chains act as the elastically effective bridge chain near C_{gel} and its number density increases with c. These results may be because the viscoelastic experiments in this study are conducted near C_{gel}, and the population of the bridge conformation will show drastic variation with the small change of concentration. As mentioned above, fairly amount of aggregates exist in the lower polymer concentration systems, but their contribution on the viscoelasticity becomes negligible with the increase of concentration. The transient network is supposed to grow by incorporating the aggregates into the macroscopic network with increasing the fraction of bridge conformation for P*t*BuA chain.

Table 1
Apparent activation energy ΔH_{app} evaluated from shift factor

Concentration (wt%)	ΔH_{app} (kJ/mol)
4.4	568
5.9	542
8.0	450
12.0	473

5. Conclusions

Systematic studies of PMMA–P*t*BuA–PMMA/1-butanol system from dilute to moderately concentrated solutions have been conducted in order to investigate the association and gelation mechanism of ABA triblock copolymer in B-selective solvent near $T_{micelle}$ and C_{gel}. Static and dynamic light scattering and ^{1}H NMR measurements for dilute solutions revealed that PMMA–P*t*BuA–PMMA chains are molecularly dissolved at high temperature. With decreasing

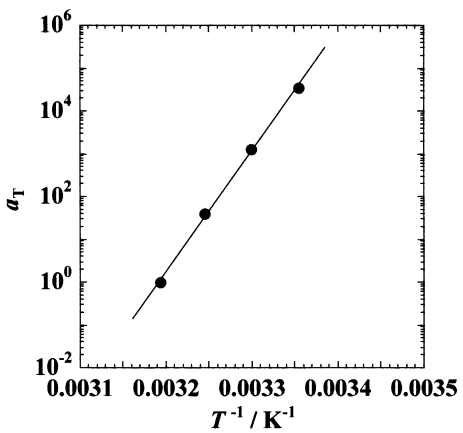

Fig. 9. Typical example of Arrehnius plot derived from the time–temperature superposition for 5.9 wt% solution.

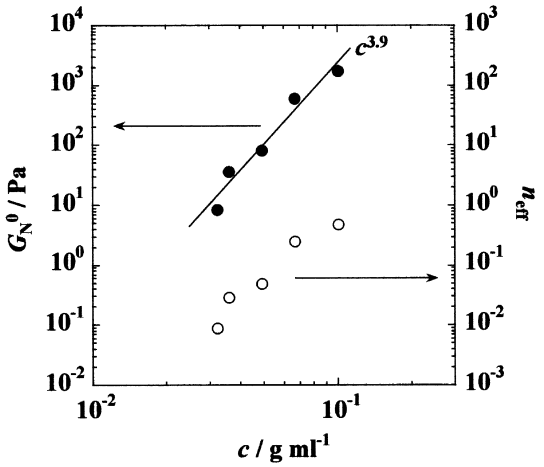

Fig. 10. Concentration dependence of the plateau modulus G_N^0 (●) and the fraction of the elastically effective chain n_{eff} (○).

temperature, the triblock copolymers form a micelle consisting PMMA associated core and P*t*BuA shells and its apparent aggregation number is ~90. Linear dynamic viscoelastic measurements for solutions with moderate polymer concentration (3.9–12.0 wt%) reveal that the system changes from viscous sol state to elastic gel state with decreasing temperature. The consistency between $T_{micelle}$ and T_{VE} indicates that the physical gelation is owing to the formation of the network structure as the result of the association of PMMA chains and the bridging P*t*BuA chains connecting the associated PMMA core. Just above C_{gel}, the viscoelasticity suggests the existence of fairy amount of aggregates not incorporated in the macroscopic network. With the increase in polymer concentration, the viscoelastic master curves derived by time–temperature superposition become to resemble the Maxwell-type modulus curve with narrow relaxation time distribution, suggesting the formation of the transient network. The scaling exponent for the plateau modulus G_N^0 against polymer concentration is evaluated as 3.9. This large value is considered to be reflecting the development of macroscopic network with the increase in polymer concentration above C_{gel}, i.e. the aggregates tend to be incorporated into the macroscopic network with increasing the fraction of bridge conformation for P*t*BuA chain.

Acknowledgements

This work was financially supported by Grant-in-Aid for Scientific Research (No. 11450364), and Grant-in-Aid for Scientific Research on Priority Areas (A), 'Dynamic Control of Strongly Correlated Soft Materials' (No. 413/13031031) from the Ministry of Education, Science, Sports, Culture, and Technology.

References

[1] Green MS, Tobolsky AV. J Chem Phys 1946;14(2):80–92.
[2] Tanaka F, Edwards SF. Macromolecules 1992;25(5):1516–23.
[3] Tanaka F, Edwards SF. J Non-Newtonian Fluid Mech 1992;43: 247–71.
[4] Tanaka F, Edwards SF. J Non-Newtonian Fluid Mech 1992;43: 273–88.
[5] Tanaka F, Edwards SF. J Non-Newtonian Fluid Mech 1992;43: 289–309.
[6] Tanaka F. Polym J 2002;34(7):479–509.
[7] Annable T, Buscall R, Ettelaie R, Whittlestone D. J Rheol 1993;37: 695–726.
[8] Annable T, Buscall R, Ettelaie R. Colloid Surf 1996;112:97–116.
[9] Tam KC, Jenkins RD, Winnik MA, Bassett DR. Macromolecules 1998;31(13):4149–59.
[10] Pham QT, Russel WB, Thibeault JC, Lau W. Macromolecules 1999; 32(9):2996–3005.
[11] Pham QT, Russel WB, Thibeault JC, Lau W. Macromolecules 1999; 32(15):5139–46.
[12] Ng WK, Tam KC, Jenkins RD. J Rheol 2000;44(1):137–47.
[13] Watanabe H, Kuwahara S, Kotaka T. J Rheol 1984;28(4):393–409.
[14] Sato T, Watanabe H, Osaki K. Macromolecules 1996;29(19):6231–9.
[15] Watanabe H, Sato T, Osaki K, Yao ML, Yamagishi A. Macromolecules 1997;30(19):5877–92.
[16] Watanabe H, Sato T, Osaki K. Macromolecules 2000;33(7):2545–50.
[17] Sato T, Watanabe H, Osaki K. Macromolecules 2000;33(5):1686–91.
[18] Raspaud E, Lairez D, Adam M, Carton JP. Macromolecules 1994; 27(11):2956–64.
[19] Raspaud E, Lairez D, Adam M, Carton JP. Macromolecules 1996; 29(4):1269–77.
[20] Lairez D, Adam M, Carton JP, Raspaud E. Macromolecules 1997; 30(22):6798–809.
[21] Vega DA, Sebastian JM, Richard YL, Register A. J Polym Sci Part B Polym Phys 2001;39:2183–97.
[22] Yu JM, Dubois Ph, Teyssié Ph, Jérôme R, Blacher S, Brouers F, L'Homme G. Macromolecules 1996;29:5384–91.
[23] Soenen H, Berghmans H, Winter HH, Overbergh N. Polymer 1997; 38:5653–60.
[24] Yamazaki R, Inomata K, Nose T. Polymer 2002;43:3647–52.
[25] Itakura M, Inomata K, Nose T. Polymer 2001;42:9261–8.